GEOLOGICAL SURVEY OF CANADA
OPEN FILE 7852

Targeted Geoscience Initiative 4: Contributions to the Understanding of Precambrian Lode Gold Deposits and Implications for Exploration

Geology of the metamorphosed Roberto gold deposit (Éléonore Mine), James Bay region, Quebec: diversity of mineralization styles in a polyphase tectonometamorphic setting

Arnaud Fontaine[1], Benoît Dubé[2], Michel Malo[1], Vicki J. McNicoll[3], Tony Brisson[4], Dominique Doucet[5], and Jean Goutier[6]

[1]Institut national de la recherche scientifique – Centre Eau Terre Environnement, Québec, Quebec
[2]Geological Survey of Canada, Québec, Quebec
[3]Geological Survey of Canada, Ottawa, Ontario
[4]Goldcorp Inc., Éléonore mine, Rouyn-Noranda, Quebec
[5]Ressources Sirios, Montréal, Quebec
[6]Ministère de l'Énergie et des Ressources naturelles, Rouyn-Noranda, Quebec

2015

Recommended citation

Fontaine, A., Dubé, B., Malo, M., McNicoll, V.J., Brisson, T., Doucet, D., and Goutier, J., 2015. Geology of the metamorphosed Roberto gold deposit (Éléonore Mine), James Bay region, Quebec: diversity of mineralization styles in a polyphase tectonometamorphic setting, *In:* Targeted Geoscience Initiative 4: Contributions to the Understanding of Precambrian Lode Gold Deposits and Implications for Exploration, (ed.) B. Dubé and P. Mercier-Langevin; Geological Survey of Canada, Open File 7852, p. 209–225.

Publications in this series have not been edited; they are released as submitted by the author.

Contribution to the Geological Survey of Canada's Targeted Geoscience Initiative 4 (TGI-4) Program (2010–2015)

TABLE OF CONTENTS

Geology of the metamorphosed Roberto gold deposit (Éléonore Mine), James Bay region, Quebec: diversity of mineralization styles in a polyphase tectonometamorphic setting

Arnaud Fontaine[1], Benoît Dubé[2], Michel Malo[1], Vicki J. McNicoll[3], Tony Brisson[4], Dominique Doucet[5], and Jean Goutier[6]

[1]Institut national de la recherche scientifique – Centre Eau Terre Environnement, 490 rue de la Couronne, Québec, Quebec G1K 9A9
[2]Geological Survey of Canada, 490 rue de la Couronne, Québec, Quebec G1K 9A9
[3]Geological Survey of Canada, 601 Booth Street, Ottawa, Ontario K1A 0E9
[4]Goldcorp Inc., Éléonore mine, 853, boulevard Rideau, Rouyn-Noranda, Quebec J9Y 0G3
[5]Ressources Sirios, 1000, rue St-Antoine Ouest, bureau 415, Montréal, Quebec H3C 3R7
[6]Ministère de l'Énergie et des Ressources naturelles, 70, avenue Québec, Rouyn-Noranda, Quebec J9X 6R1
*Corresponding author's e-mail: arnaud.fontaine@ete.inrs.ca

ABSTRACT

The world-class Roberto gold deposit is a major discovery in the James Bay region. Hosted by <2675Ma (Timiskaming) sedimentary rocks, the deposit is located a few kilometres south of the tectonometamorphic contact between the Opinaca (paragneiss to migmatite) and the La Grande subprovinces (tonalitic basement, volcano-sedimentary belts and syn- to late-tectonic intrusions). Multiple deformation events, long-lived metamorphic event(s), and magmatic activity, including proximity to the migmatitic Opinaca domain, constitute a geological context that is favourable for long-lived hydrothermal systems or multiple mineralizing and/or remobilization events.

Detailed underground and surface mapping of the ore zones and host rocks of the Roberto gold deposit (Éléonore mine) provide new insights into host-rock variations, relationships between metamorphism and ore zones, syn- to post-mineralization structural events, and magmatic activity. These have led to a diversity of mineralization styles including i) stockwork of quartz, dravite (magnesian tourmaline) veinlets with microcline, phlogopite replacement zones with pyrrhotite, arsenopyrite, and löllingite (Roberto zone), ii) quartz, diopside, schorl (iron-rich tourmaline), arsenopyrite veins (East-Roberto zone), and iii) more atypical ore zones in migmatitic rocks or in biotite, amphibole schist (Lake zone). All of the mineralized zones are deformed (isoclinal folding, mylonitic shearing, boudinage) and some (e.g. Roberto zone) are locally strongly metamorphosed, suggesting that the bulk of the ore is pre-peak metamorphism (amphibolite facies). The timing of the mineralization relative to peak metamorphism and the complex geological setting are the dominant factors that influenced the nature of the Roberto deposit.

INTRODUCTION

Gold deposits located in deformed and metamorphosed terranes are associated with a wide range of host rocks originating from various crustal levels. Polyphase deformation and metamorphism have often obscured the primary characteristics and genetic history of these deposits (Poulsen et al., 2000; Goldfarb et al., 2005; Robert et al., 2005; Dubé and Gosselin, 2007 and references therein). Although most of these deposits occur in greenschist-facies metamorphic rocks (e.g. Hodgson, 1993; Groves et al., 1998; Goldfarb et al., 2005; Robert et al., 2005), some are also found in amphibolite and granulite metamorphic terranes (Barnicoat et al., 1991; McCuaig et al., 1993; Neumayr et al., 1993; Kisters et al., 1998; Dubé et al., 2000; Dubé and Gosselin, 2007). The temporal relationship between gold deposition and peak metamorphism is a critical feature to define metamorphic/hydrothermal processes, often involved in the genesis of gold deposits in these high-grade metamorphic terranes (Stüwe, 1998; Poulsen et al., 2000; Tomkins and Mavrogenes, 2002; Tomkins et al., 2004, 2006; Phillips and Powell, 2009). High metamorphic gradients, roughly coincident with large-scale tectonic contacts may represent important criteria for gold exploration (e.g. Thompson, 2003; Gauthier et al. 2007).

The world-class Roberto gold deposit is a relatively recent discovery in the less explored James Bay region with reserves of 4.97 Moz at 6.3 g/t Au, measured and indicated resources of 1.06 Moz at 6.34 g/t Au, and

Fontaine, A., Dubé, B., Malo, M., McNicoll, V.J., Brisson, T., Doucet, D., and Goutier, J., 2015. Geology of the metamorphosed Roberto gold deposit (Éléonore Mine), James Bay region, Quebec: diversity of mineralization styles in a polyphase tectonometamorphic setting, *In:* Targeted Geoscience Initiative 4: Contributions to the Understanding of Precambrian Lode Gold Deposits and Implications for Exploration, (ed.) B. Dubé and P. Mercier-Langevin; Geological Survey of Canada, Open File 7852, p. 209–225.

inferred resources of 2.80 Moz at 7.19 g/t Au (Goldcorp, 2014).

Previous work (Ravenelle et al., 2009, 2010; Ravenelle, 2013) on the Roberto deposit mainly focussed on the detailed surface mapping of the large stripped Roberto outcrop, supplemented by drill-core descriptions, U-Pb geochronology, and gOcad 3-D modeling, which uncovered the complex structural pattern, stratigraphic relationships, alteration assemblages, and timing of gold mineralization. Such a complex setting complicates the study of the genesis of the deposit and the definition of its geological and hydrothermal footprints.

The current project is part of a Ph.D. study by the first author, in progress at the Institut national de la recherche scientifique, Centre Eau Terre Environnement (INRS ETE) in collaboration with the Geological Survey of Canada (GSC), Goldcorp Inc. Éléonore Mine and Géologie Québec, under the umbrella of the Targeted Geoscience Initiative 4 - Lode Gold project of Natural Resources Canada (Dubé et al., 2011a). The study uses a multidisciplinary approach focussing on extensive detailed underground mapping, structural analysis, core logging, lithogeochemical analysis, U-Pb geochronology, and petrography to establish the various geological characteristics and processes involved in the genesis of the Roberto gold deposit. The main goal of this report is to provide an overview of the underground geology of the Roberto deposit.

REGIONAL GEOLOGY

The Superior Province is one of the most gold-rich Archean cratons with more than 375 Moz Au of estimated gold (Gosselin and Dubé, 2005a,b; B. Dubé and V. Bécu, unpub. data). The James Bay region is part of the Superior Province of the Canadian Shield (Card and Ciesielski, 1986; Percival et al., 2007), which is characterized by Neoarchean rocks with Meso- and Paleoarchean reworked domains (3.45–2.57 Ga; Goutier and Dion, 2004). The metamorphic grade increases quickly to the granulitic metasedimentary units of the Opinaca subprovince, which is interpreted as an injection complex (Morfin et al., 2013). Migmatization of the sedimentary rocks occurred between 2663 and 2637 Ma (Morfin et al., 2013). The La Grande subprovince comprises sedimentary rocks, local volcanic assemblages, and numerous intrusions (Franconi, 1978; Goutier et al., 2001; Moukhsil et al., 2003), underlain by an older Archean basement (Goutier et al., 2001; Bandyayera et al., 2010). The contact between the two subprovinces defines the first-order gold metallotect in the James Bay area as most known gold deposits and showings are located within about few kilometres of this contact (Fig. 1a), such as the Corvet-Est (Aucoin et al., 2011), the La Grande-Sud (Mercier-Langevin et al., 2012), and the turbidite-hosted Wabamisk (Beauchamp et al., 2015) projects. Since the discovery of the Roberto deposit by Mines d'or Virginia in 2004, this contact and, in particular, the adjacent polydeformed turbiditic basins are the current exploration targets in the James Bay region (Gauthier, 2000; Gauthier et al., 2007; Ravenelle et al., 2009, 2010; Ravenelle, 2013).

GEOLOGICAL SETTING OF THE DEPOSIT

Located near the boundary between the La Grande and Opinaca subprovinces, the deposit is hosted by a polydeformed <2675Ma (Timiskaming) turbiditic sequence, metamorphosed to amphibolite facies (Ravenelle et al., 2009, 2010; Ravenelle, 2013; Fontaine et al., 2014, and this study). The main part of the Éléonore property (La Grande subprovince, Fig. 1b) is composed of syn- to late-tectonic granodiorite, tonalite, diorite, and pegmatite, intruding the volcanic and sedimentary units of the Kasak and Low formations (Bandyayera and Fliszár, 2007). The Réservoir Opinaca pluton (Fig. 1b) is a polyphase intrusion composed of an early tonalitic phase (2708.9 ± 0.9 Ma: David et al., 2009) and a late dioritic phase (2703.5 ± 2.8 Ma: David et al., 2009). The Lac Ell intrusion (2705.6 ± 1.9 Ma: J. David, 2005) hosts Au-Ag-Cu-Mo mineralization (Bécu et al., 2007; Ravenelle et al., 2010). Pillowed lava and lapilli tuff of the Kasak Formation (2704 ± 1.1 Ma: Bandyayera and Fliszár, 2007) are unconformably overlain by <2702 ± 3 Ma polymictic clast-supported conglomerate (locally termed "ALow1"), which marks the base of the Low Formation (for details, see Ravenelle et al., 2010). Stratigraphically above, the turbiditic part of the Low Formation (termed "ALow2"; Bandyayera and Fliszár, 2007) comprises decimetre- to metre-thick lenses of arenite interbedded with an aluminosilicate-bearing greywacke. Detailed U-Pb work of the Low Formation in the Roberto deposit area has unravelled a structurally inverted stratigraphy involving an older sedimentary assemblage consisting of <2714 Ma massive greywacke (Ravenelle et al., 2010) intercalated with <2697 Ma aluminosilicate-bearing greywacke (Ravenelle, 2013) lying structurally above a younger sedimentary assemblage characterized by thinly bedded greywacke dated at <2675 Ma (Ravenelle et al., 2010) interbedded with massive greywacke. The gold mineralization is mainly hosted within the <2675 Ma thinly bedded greywacke at the top of the Low Formation (ALow2; Ravenelle et al., 2010). These sedimentary rocks are intruded by pegmatite dykes (Figs. 1, 2), and locally gradually evolve into paragneiss or migmatite towards the contact with the Opinaca subprovince (for details, see Ravenelle et al., 2010).

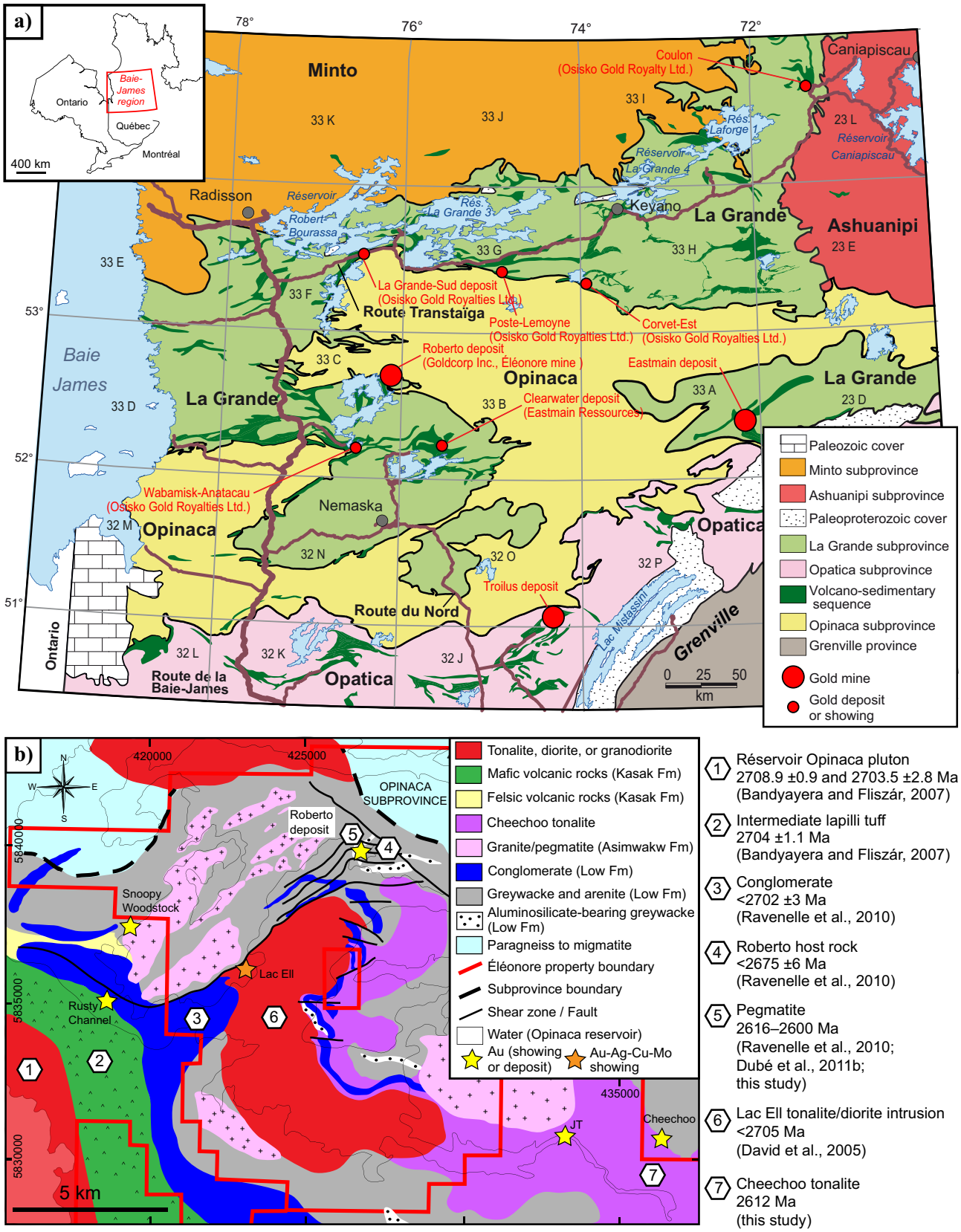

Figure 1. a) Simplified lithotectonic map of the James Bay region (modified after Thériault and Beauséjour, 2012; J. Goutier, 2014, work in progress). **b)** Geology of the Éléonore property with the location of the deposit/mine and geochronological data illustrating the complex tectonometamorphic framework and magmatic events associated with the Roberto gold deposit (modified after Bandyayera et al., 2010; Ravenelle et al., 2010; Ravenelle, 2013; and this study). Abbreviation: Fm = formation. Geographical coordinates: NAD83, UTM zone 18N.

STRUCTURAL FEATURES

Three main phases of regional deformation are recognized in the study area (Bandyayera and Fliszár, 2007; Bandyayera et al., 2010; Ravenelle et al., 2010; Ravenelle, 2013). The regional D_1 deformation consists of rare intrafolial folds, oriented north-northeast (Bandyayera and Fliszár, 2007). D_2 is the main phase of deformation associated with regional metamorphism. It is characterized by an east- to southeast-trending S_2 foliation associated with tight to isoclinal F_2 folds with steeply plunging hinge lines. An associated subvertical L_2 mineral lineation (biotite, aluminosilicate porphyroblasts) is preferentially present in aluminosilicate-bearing greywacke and conglomerate (Bandyayera et al., 2010; Ravenelle et al. 2010; this study). An S_3 crenulation cleavage locally reorients syn-D_2 metamorphic minerals (e.g. biotite, fibrous sillimanite, K-feldspar). F_3 folds have centimetric to metric wavelengths and are generally more open than F_2 folds (Bandyayera et al., 2010; Ravenelle et al., 2010; this study) and their interaction produces Type 3 fold interference patterns (Ramsay and Huber, 1987; Ravenelle, 2013). Ravenelle et al. (2010) have also documented sheath folds, which they interpret as related to the effect of continuous ductile deformation along D_2 high-strain zones on early F_2 folds.

At deposit scale, D_1 deformation is inferred by the repetition of the aluminosilicate-bearing greywacke along the southern limb of a kilometre-scale F_2 fold (Ravenelle et al., 2013). Although no evidence of D_1 deformation was observed in the 410 mine level (Fig. 2), the strongly deformed interbedded greywacke could be affected by early deformation event(s), as observed by the local presence of F_1 folds in the area close to the deposit (Ravenelle, 2013). The latter is characterized by a steeply dipping, roughly west-trending axial planar S_2 foliation, well displayed by the alignments of aluminosilicate porphyroblasts or biotite. These minerals define the L_2 lineation, commonly colinear with F_2 fold axes. F_2 folds are steeply plunging to subvertical and are commonly non-cylindrical and disharmonic. A steeply dipping northwest-trending S_3 crenulation cleavage locally deforms the S_2 foliation and is associated with non-coaxial strain reactivation of D_2 high-strain zones. The <2675 Ma thinly bedded greywacke (Fig. 3a) is strongly deformed by D_2 and D_3 fabrics on mine levels 410 and 380 (Figs. 2, 4). Similar deformation and chronology of events have been recorded by the quartzo-feldspathic veins in paragneiss, exposed 1 km east of the deposit. Two structural domains have been defined on the 410 mine level (Fig. 2): a southern domain, dominated by east-trending tight to isoclinal F_2 folds, where bedding is well preserved; and a northern domain dominated by a strongly developed S_3 crenulation cleavage axial planar to northeast-trending F_3 folds. The northern and southern domains are separated by D_2 high-strain zones. The latter may have been reactivated during D_3 deformation. Three structural domains are also defined based on the relative orientation of bedding versus S_2 foliation. A western domain is characterized by northwest-trending bedding though S_2 foliation is east-trending (Fig. 2, stereoplot 1). The central domain is marked by an irregular orientation of S_2 foliation (Fig. 2, stereoplot 2) probably related to the emplacement of pegmatitic material or F_3 folding (Fig. 2). Lastly, the eastern domain display S_2 foliations and bedding that are parallel to the east (Fig. 2, stereoplot 3) and is interpreted to be related to strong D_2 transposition along the contact of the aluminosilicate-bearing greywacke (< 2697 Ma) with the interbedded and more competent greywacke unit. This zone of strong transposition is well exposed on the large surface-stripped outcrop (Fig. 2b), although in some areas the original north-south orientation of the bedding is preserved (for details, see Ravenelle et al., 2010). Some of these D_2 high-strain zones contain elongated clasts of granitic pegmatite (e.g. near exploration shaft; Fig. 2) suggesting that these pegmatite units were intruded before or during D_2 deformation. These steeply dipping (79–88°) west to southwest-trending (N280°–N220°) high-strain zones intersect the east-trending and south-dipping orezone lenses located in the hanging wall of the main Roberto and Roberto East zones (Fig. 2).

Post-D_3 northwest- to east-trending conjugates sets of brittle faults (N310º and N340°) are marked by a coating of chlorite, epidote, and locally calcite and chalcopyrite and contain brecciated material with angular fragments of host rocks. Displacement along those late brittle faults ranges from a few centimetres to several metres and commonly shows brecciated material with angular fragments of the host rocks.

METAMORPHISM

Sedimentary rocks of the Low Formation (Fig. 3a,b) underwent prograde amphibolite-facies metamorphism, which sharply increases towards the contact with the Opinaca subprovince, as illustrated by the presence of (i) aluminosilicate (sillimanite), muscovite and K-feldspar porphyroblasts in metapelitic rocks, (ii) amphibole or biotite porphyroblasts in greywacke (Fig. 3c), (iii) an increasing proportion of quartzo-feldspathic veinlets with residual biotite selvages in greywacke, and (iv) paragneiss (Fig. 3d). Centimetre-sized amphibole porphyroblasts locally occur in the host rocks (Fig. 3c), near contacts with granitic pegmatite or feldspar-phyric monzonite (Fig. 3e,f). In the deposit area, the metamorphic gradient increases rapidly toward the northeast and with depth. These features suggest that isograds are probably southeast-trending with moderate dips of 45° to the southwest. In

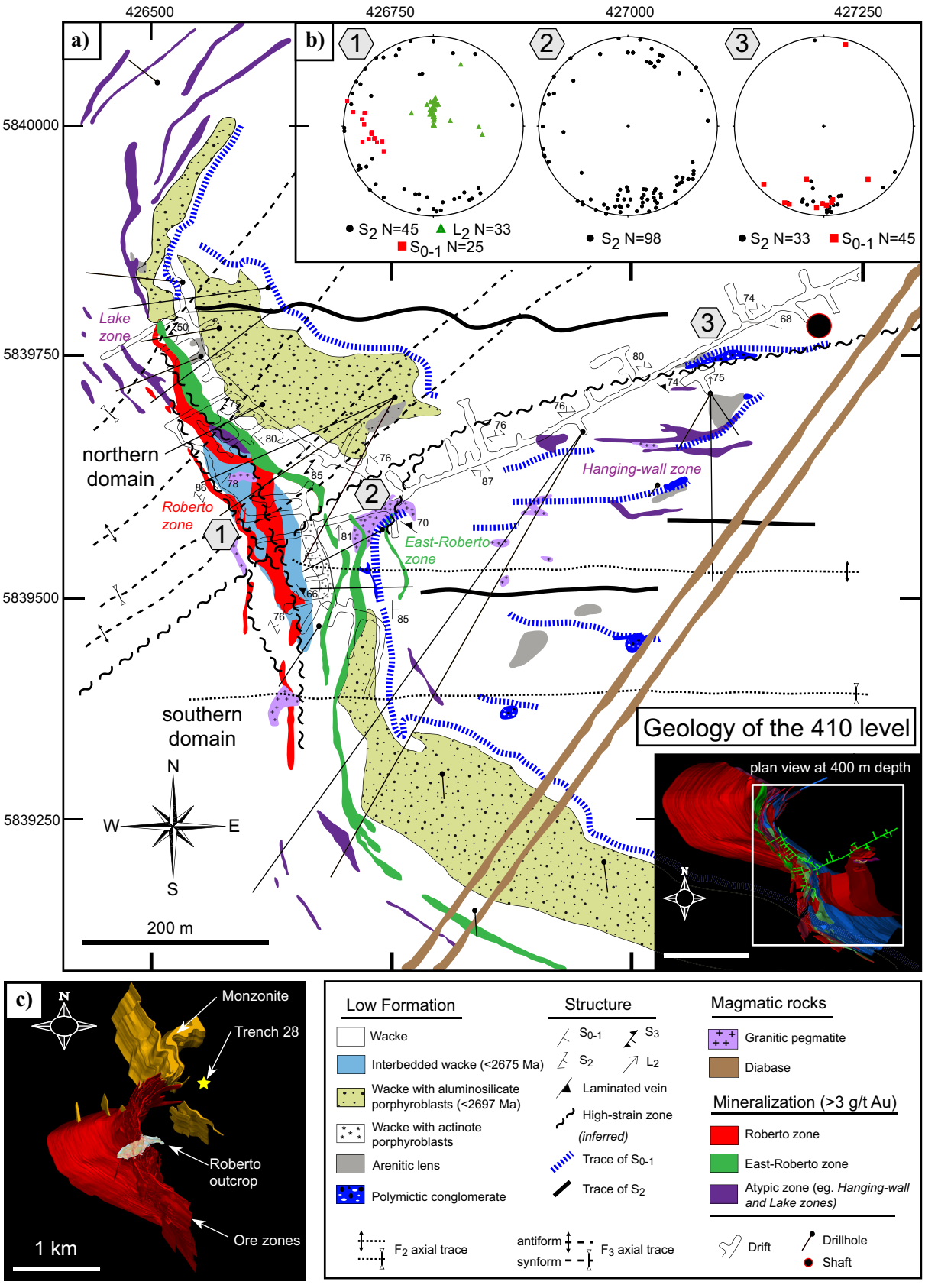

Figure 2. a) Simplified geological map of the 410 level (390 m depth) with main rock types and structures. **b)** Stereographic projections of fabrics associated with structural domains. **c)** Illustration of the geological model of the Roberto deposit with the location of Trench 28, monzonite, ore zones, Roberto outcrop, and Trench 28 (for details, see Fig. 6). Geographical coordinates: NAD83, UTM zone 18N.

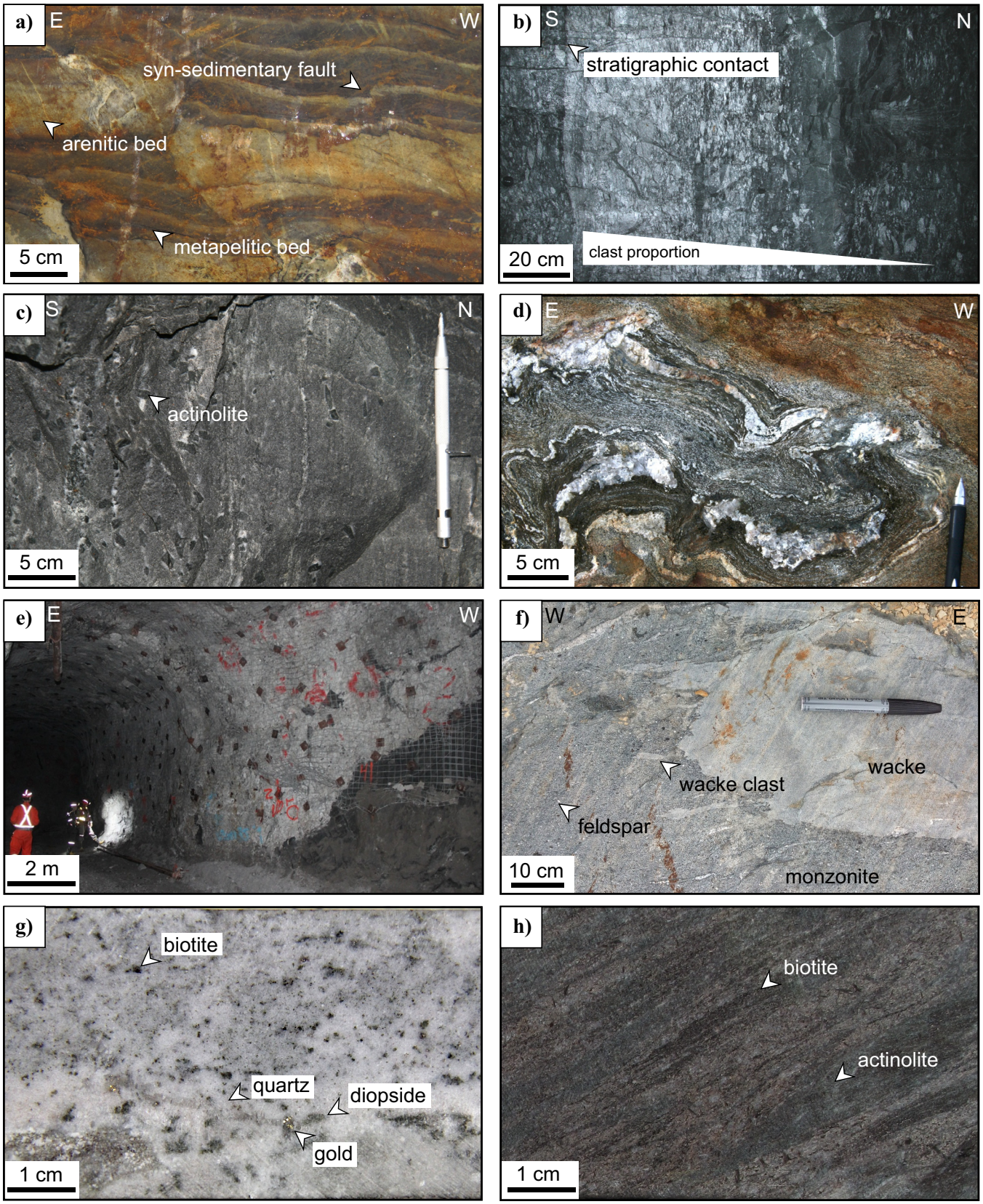

Figure 3. Photographs of **a)** interbedded greywacke with syn-sedimentary faults in the Trench 28; **b)** polymictic conglomerate (west wall at 600 m depth), facing north; **c)** amphibole-porphyroblasts wacke; **d)** paragneissic rocks; **e)** granitic pegmatite (at 400 m depth); **f)** monzonitic rocks; **g)** Cheechoo tonalite mineralization (photograph by Benoît Dubé, 2014; drillhole CH-919-12; 25.9 g/t Au, 136–137 m); and **h)** Lake Zone (biotite, amphibole schist).

some cases where partial melting occurred, residual biotite is present in association with hornblende in rims of quartzo-feldspathic veins (Fig. 3d).

Prograde metamorphism results in the breakdown of muscovite and growth of K-feldspar porphyroblasts (e.g. in the aluminosilicate-bearing greywacke) at depth possibly following the muscovite + quartz = K-feldspar + sillimanite + H_2O metamorphic reaction (Ravenelle, 2013). That reaction probably precludes migmatization in the stability field of the biotite, i.e., at a temperature of <800°C (Vielzeuf and Holloway, 1988) with the muscovite + plagioclase + quartz = melt + sillimanite + biotite melting reaction (Thompson and Tracy, 1979). This is well illustrated in a trench (Fig. 3d), where quartz-feldspar subparallel veinlets are associated with biotite, hornblende residual material in veinlet selvages.

Various generations of metamorphic and hydrothermal biotite are documented using petrography and mineral chemistry (#Mg versus Al^{iv}). Three preliminary groups are recognized: i) metamorphic biotite in metapelite and in the rims of K-feldspar, muscovite, sillimanite porphyroblasts (group 1), ii) residual biotite in paragneiss (group 2), and iii) hydrothermal phlogopite in pervasive calcium-bearing hydrothermal assemblages (group 3). Biotite thermometry data using titanium contents (Henry et al., 2005) of the first group (F ranging from 0.103 to 0.272 apfu) in metapelite of the interbedded greywacke gave metamorphic temperatures ranging from 542 to 705°C (RSD of 7.4% for n=32) with a mean value of 650 ± 16°C. This result is corroborated by preliminary garnet-biotite thermometry (Holdaway, 2000) data of biotite inclusions within M_2 garnet porphyroblasts in garnet-bearing sedimentary rocks found in the northern part of the deposit, which yielded a temperature estimate of 657°C.

MAGMATISM

Granitic, lithium-cesium-tantalum-enriched (LCT) pegmatite (Černý, 1991; Černý and Ercit, 2005), dated between ca. 2620 and 2600 Ma (U-Pb zircon age; Ravenelle et al., 2010; Dubé et al., 2011b; this study), occur as centimetric to metric dykes (Figs. 2, 3e) that locally display progressive transition with quartzo-feldspathic and quartz veins (Ravenelle, 2013; this study). Quartz and feldspar are present in various proportions in association with schorl, garnet, and rare traces of spodumene. Miarolitic cavities contain quartz, schorl, and spodumene crystals. Alkali feldspar and quartz occasionally show skeletal or graphic intergrowths. Coarse-grained quartz ± schorl-bearing dykes were injected within feldspar-garnet aplitic domains. They are commonly boudinaged and isoclinally folded (Ravenelle et al., 2010). U-Pb ages of these pegmatite dykes range from 2616 to 2603 Ma (Ravenelle, 2013). Furthermore, gold-bearing ca. 2600 Ma (ID-TIMS U-Pb preliminary age) granitic pegmatite located in the North zone (see below) contains acicular centimetric arsenopyrite-löllingite crystals in quartz-rich domains.

A feldspar-phyric monzonite sill (Fig. 2b), with a maximum age of ca. 2674 Ma, is mapped a few hundred metres north of the main ore zones, in the western part of the North zone (for details, see Alteration and Mineralization below). This intrusion (Fig. 3f), which displays irregular contacts with the host greywacke, is composed of quartz, amphibole, and biotite with local traces of pyrite, pyrrhotite, diopside, and rounded to elongated clasts of host rocks (e.g. greywacke, amphibolite, arenite). The monzonite is foliated by the S_2 fabric. A foliated feldspar porphyry intermediate dyke (~5 m wide) mapped next to the exploration shaft contains disseminated fine-grained pyrite and has a maximum U-Pb age of ca. 2688 Ma.

A tonalite intrusion that hosts the Cheechoo gold project (Fig. 1b; Ressources Sirios, 2014) is composed of local feldspar phenocrysts in a matrix of quartz, albite An_{10} microcline, biotite, and rare traces of diopside and actinolite. Preliminary petrographic and lithogeochemical data indicate that the intrusion is locally of granodioritic composition. The intrusion, locally cut by a stockwork of quartz veinlets, is deformed, recrystallized, and foliated, as shown by elongated biotite and chlorite. Textures vary from aplitic, granoblastic, gneissic, to nematoblastic. Locally, the tonalite evolves progressively to quartz-feldspar pegmatite dykes. The pegmatite dykes locally comprise strongly foliated amphibole- and biotite-rich mafic and greywacke clasts that contain traces of diopside, disseminated fine-grained arsenopyrite, pyrrhotite, and gold. The tonalite is the main host to the auriferous zones and drillhole intersections grade up to 7.24 g/t Au over 7.9 m (Ressources Sirios, 2014). The auriferous tonalite is silicified and/or K-altered, Na-altered and contain traces of disseminated fine-grained arsenopyrite and pyrrhotite and local quartz veinlets. Undeformed quartz-feldspar pegmatite is also locally auriferous. Visible gold locally occurs in grey quartz replacement zones or within quartz veinlets (Fig. 3g). A preliminary zircon age of ca. 2612 Ma (U-Pb Isotope Dilution Thermal Ionization Mass Spectrometry (ID-TIMS)) for the Cheechoo intrusion is interpreted as the crystallization age. This age is contemporaneous with some auriferous zones of the Roberto deposit dated at ca. 2615 to 2607 Ma (Ravenelle et al., 2010) and provide a maximum age for this phase of gold mineralization.

ALTERATION AND MINERALIZATION

The ore zones at Roberto are associated with a relatively large hydrothermal system characterized by a proximal potassium- to magnesium-bearing metaso-

matic alteration halo (0–75 m from ore zones; Fig. 4b) surrounded by an intermediate (75–100 m; Fig. 4e) or distal calcium-bearing alteration halo (≤100–250 m; Fig. 4c,f). From distal to proximal, the calcium-bearing metasomatism is characterized by replacement bands or diffuse zones with calcium-rich minerals (actinolite, diopside) in association with feldspar (20–60%), actinolite (25–30%), and a minor amount of coarse-grained biotite and quartz (Fig. 4e). Metasomatic layers/zones (Fig. 4f) are locally zoned with coarser minerals, suggesting open-space filling or possible recrystallization of the mineral phases during the prograde metamorphism (Fig. 4b,f). Diffuse replacement zones are characteristic of the distal hydrothermal footprint. The proportion of diopside and tourmaline (mainly schorl) strongly increases in proximity of ore zones (Ravenelle al., 2010). Also, the abundance and thickness of metasomatic material (e.g. replacement zones, veins, and veinlets) and deformation intensity also increase in the vicinity of high-grade zones (e.g. Roberto and East-Roberto). For example, veinlet networks evolve sharply to pervasive silica flooding with tourmaline enrichment approaching the East-Roberto zone. The presence of centimetric porphyroblasts of actinolite, phlogopite, and arsenopyrite, in association with microcline replacement zones and stockwork of quartz, dravite (magnesian tourmaline), are typical features of the proximal metasomatic alteration (Fig. 4b,c).

Several styles of mineralization have been documented from surface (Ravenelle, 2010) and underground mapping (this study). The Roberto stripped outcrop (Fig. 2b) exposes the richest domains of the gold mineralization (for details, see Ravenelle et al., 2010 and Ravenelle, 2013) where ore zones are preferentially hosted in thinly bedded greywacke adjacent to non-economic to barren massive greywacke. The Roberto style of mineralization (up to 25 g/t Au on 20 m) constitutes the bulk of the ore (Figs. 4b, 5d) and is characterized by a stockwork of quartz-sulphide veinlets and reddish-brown replacement zones (Ravenelle et al., 2010). The quartz-sulphide veinlets can form a chaotic (randomly oriented) stockwork/breccia in the massive greywacke or can be subparallel or at a high angle to the folded bedding in the interbedded greywacke. Biotite and dravite, in association with phlogopite and microcline, form replacement zones associated with the quartz-sulphides stockwork (Figs. 4d, 5a). Arsenopyrite, löllingite, and pyrrhotite (with gold inclusions) are present in the quartz-sulphide veinlets or as fine-grained disseminations in the replacement ore (Ravenelle et al., 2010). At depth, the Roberto zone is characterized by (i) an increasing proportion of microcline alteration in the selvages of the quartz-sulphide veinlets and in the matrix of the replacement ore (Fig. 4b); (ii) saccharoidal quartz ± feldspar; and (iii) recrystallized randomly oriented coarse-grained phlogopite porphyroblasts (Fig. 4b).

The East-Roberto zone (Fig. 5b,e) forms the eastern portion of the north-south mineralized corridor (Fig. 2a) and is characterized by massive or laminated quartz-diopside veins associated with silicification of host rocks, schorl veinlets, and disseminations of arsenopyrite. Underground, the East-Roberto mineralization appears spatially associated with silicified arenite lenses and local polymictic conglomerate (Fig. 5b).

Other mineralized zones of the Roberto deposit include the Lake, Hanging wall (Figs. 2a, 5c), and North zones (Fig. 6). These constitute an interesting but much smaller percentage of the deposit and result in ambiguous interpretations of ore process and genesis, most probably because of post-ore deformation and metamorphism. For instance, ore-bearing paragneiss shows progressive evolution to quartzo-feldspathic pegmatitic material (Ravenelle et al., 2010). The Lake zone is hosted by chlorite-amphibole-biotite schist (Fig. 3h) situated in the northern part of the main ore corridor. Along the northern limb of the F_2 fold, there is much higher strain intensity (Fig. 2). The Hanging-wall ore zones (Figs. 2, 5c) are located adjacent to D_2 high-strain zones and oriented subparallel to oblique to the overall trend of the S_2 foliation. They are characterized by quartz veins and local brecciated veins with pyrite, pyrrhotite, arsenopyrite and visible gold (up to 18.8 g/t over 9.6 m). Alteration assemblages around these veins share some similarities with the alteration associated with the East-Roberto and Roberto zones, suggesting similar gold-bearing fluids originating from a common deformed and metamorphosed hydrothermal system.

The North zone (Figs. 4f, 6), which is well exposed in Trench 28, is characterized by an up to 200 m thick "low-grade" envelope (1.3 g/t over 200 m). Located along the north limb of a kilometre-scale F_2 fold, the sedimentary sequence hosting the zone is mainly north-facing (Fig. 6); however, the bedding locally trends to the north, probably due to local parasitic folding. The S_2 metamorphic foliation is oriented northwest and was re-oriented by F_3 gentle to open folds. Gold mineralization occurs along the contact between the aluminosilicate-bearing greywacke and massive greywacke and within the interbedded greywacke (Fig. 6a). Exposed lithologies in Trench 28 include, from south to north, massive greywacke, overlain by aluminosilicate-bearing greywacke and interbedded greywacke (Fig. 6). Quartz-feldspar veins and veinlets lie parallel to the bedding (oriented north-south) or S_2 foliation (oriented north-west) in the aluminosilicate-bearing greywacke. The main ore zone, roughly oriented east-west, is composed of calcium-bearing mineral assem-

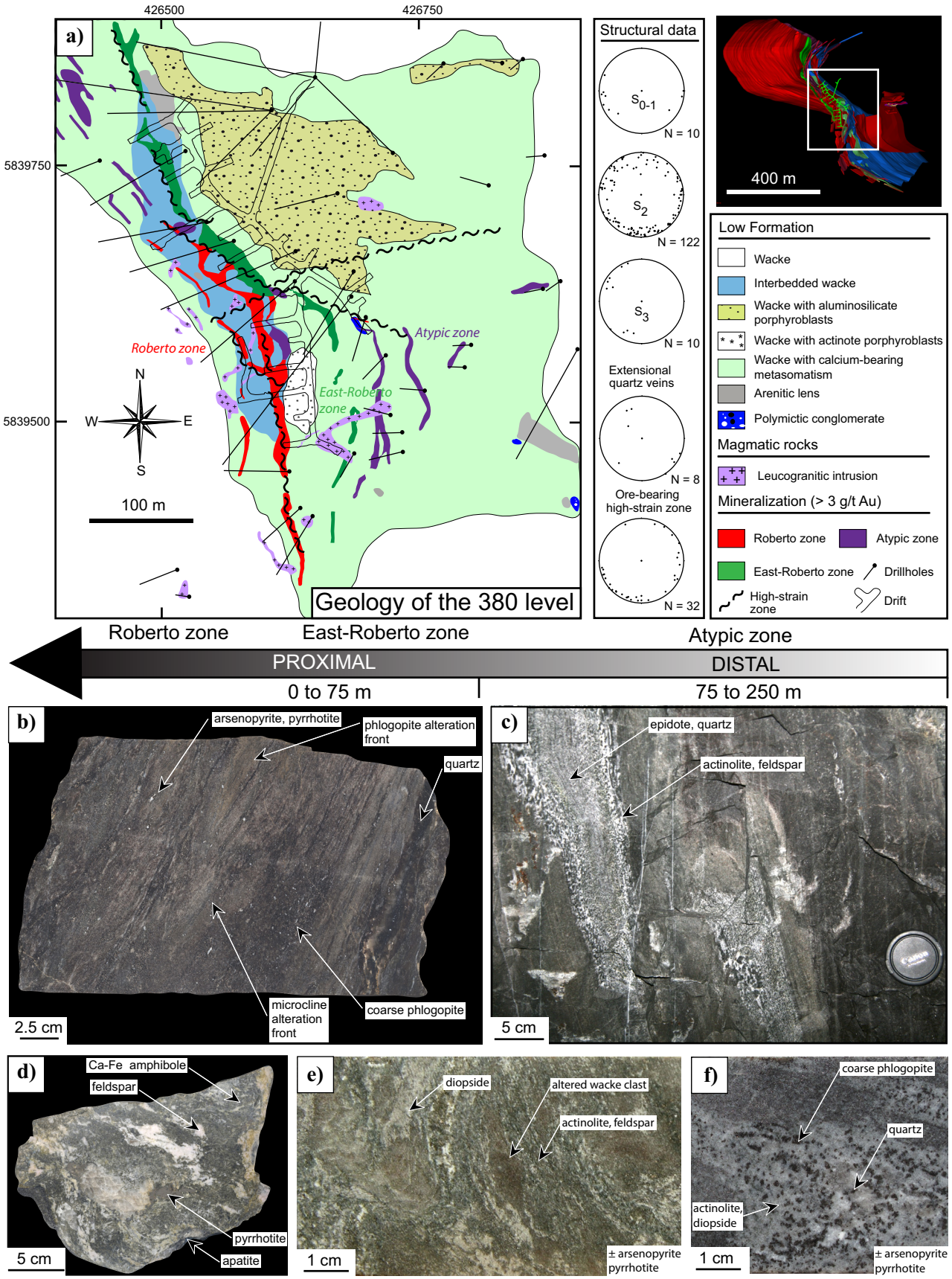

Figure 4. a) Geological map of the 380 level with stereographic projections of main structures. **b to f)** Photographs showing typical hydrothermal rocks, illustrating the zonality approaching main ore zones (East-Roberto and Roberto zones), separated into proximal (0–75 m), intermediate (75–100 m) and distal (>100–250 m). Geographical coordinates: NAD83, UTM zone 18N.

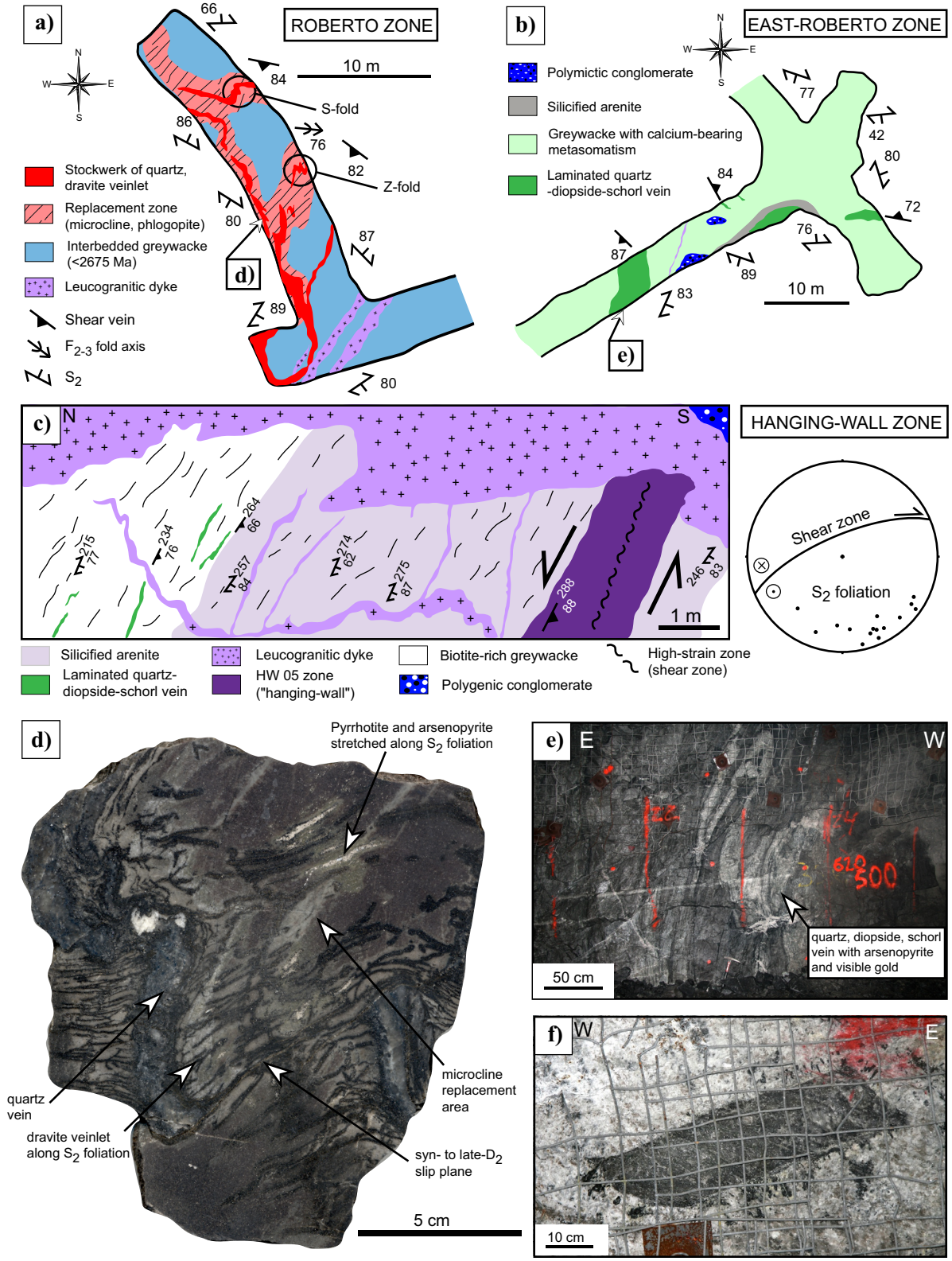

Figure 5. Simplified geological maps of **(a)** the Roberto zone (at 400 m depth) and **(b)** the East-Roberto zone (at 600 m depth). **c)** Vertical section map of the hanging-wall zone (at 600 m depth) and stereographic projections of average shear zone orientation (N=7) and S_2 foliation poles. **d)** Hand-sample showing the deformation affecting the Roberto zone. Dravite veinlets are transposed along the S_2 foliation though the quartz vein is not totally reoriented. The pyrrhotite and arsenopyrite aggregates have roughly the same structural position as the hanging-wall zones. **e)** Underground photograph of the south wall of the isoclinally folded East-Roberto zone (at 600 m depth; location highlighted in b) with several quartz generations in association with visible gold (236 g/t Au over 1 m). **f)** Underground photograph of the north wall (at 400 m depth; location highlighted in a) of the Roberto zone clast within a pegmatite that cuts across the Roberto zone.

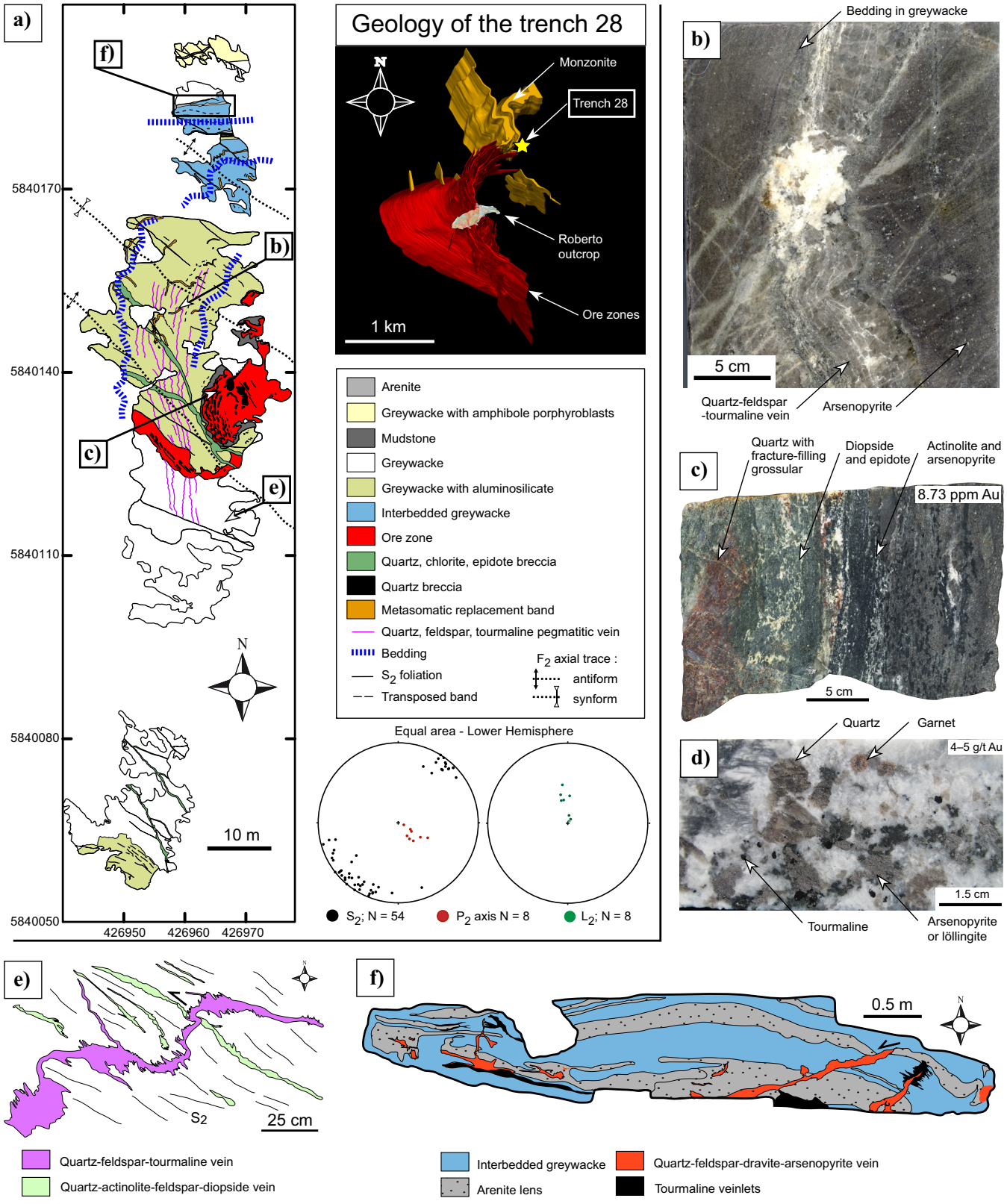

Figure 6. a) Geology of Trench 28. Note the locations of parts b, c, e, and f. Geographical coordinates: NAD83, UTM zone 18N. **b)** Quartz, feldspar, arsenopyrite-bearing vein (location highlighted in a). **c)** Hand sample of the calcium-bearing hydrothermally altered wacke in the middle of the trench (also called the Garnet Zone due to the presence of grossular). **d)** Gold-bearing pegmatite with garnet, schorl, and arsenopyrite (or löllingite). **e)** Sketch showing crosscutting relationships (see location in map a), which indicate that a quartz-feldspar-schorl vein cutting a quartz-actinolite-feldspar-diopside vein and suggesting apparent sinistral shearing along D_2-related high-strain zones. **f)** Simplified geology of the north part of the trench (see map a for location) with interbedded greywacke and decimetric arenitic lenses associated with quartz, arsenopyrite, schorl-bearing veins.

blages (grossular, diopside, carbonate, actinolite, and epidote) and disseminated coarse-grained arsenopyrite and pyrrhotite (Fig. 6c). Auriferous pegmatite dykes, locally documented in the North zone, have been intercepted in a drillhole beneath Trench 28 (19.15 g/t Au over 1.5 m). These pegmatite dykes (Fig. 6d) are zoned with feldspar-chlorite-rich walls with a predominance of quartz, feldspar, arsenopyrite, and löllingite in the cores. Such zoning, in particular quartz, feldspar, arsenopyrite, and löllingite, is interpreted to control the gold content. As this pegmatite was emplaced in barren sediment, its high gold content is not interpreted as a product of local gold remobilization but due to a magmatic gold-bearing event and/or to magma contamination during intrusion.

Most ore zones of the Roberto deposit are strongly deformed, north-trending, and located within the hinge zone of a non-cylindrical F_2 fold (Figs. 2, 4; Ravenelle et al., 2010). The geology of the north limb is more complex, as it is influenced by the presence of the monzonitic sill and the mineralized North zone. This zone, following stratigraphic contact, is strongly boudinaged and folded by F_2 and F_3 (Fig. 6a). For analogy, multiple strain increments are superimposed on the Roberto East ore zones and high-grade quartz veins have recorded isoclinal F_2 folding (Fig. 5e). On the Roberto stripped outcrop, the East-Roberto ore zone is deformed by late-D_2 oblique-dextral shearing (Ravenelle, 2013) along a steeply east-dipping high-strain zone or brittle fault with an apparent reverse component of motion, a feature that is not yet documented in underground drifts.

DISCUSSION

The main ore zones (Roberto and Roberto-East) are deformed by the main phase of deformation (D_2). This is illustrated by F_2 folds and late-D_2 slip planes deforming the Roberto stockwork (Fig. 5d), and by a S_2-foliated high-grade quartz vein of the East-Roberto mineralization isoclinally folded by F_2 (Fig. 5e). Clasts of foliated Roberto ore are found in an undeformed pegmatite cutting the main ore zone in the south part of the 410 mine level (Fig. 5f) attesting that the bulk of the mineralization was formed and deformed before the emplacement of the pegmatite. Mineralization and associated proximal alteration (e.g. diopside, microcline, phlogopite, schorl, dravite, and pyrrhotite) zones have recorded regional prograde and locally contact metamorphism. The metamorphic paragenesis and textures include (i) saccharoidal quartz in veins, (ii) biotite porphyroblasts, (iii) coarse-grained texture, and (iv) the increase of microcline alteration with depth and proximity of pegmatite. The presence of löllingite in the core of arsenopyrite (Ravenelle, 2013) and the coarse part of calcium-bearing assemblage also strongly supports the interpretation that the deposit has been metamorphosed.

The extensive magmatic activity in the study area is illustrated by several intrusive suites of tonalite (e.g. Cheechoo, Réservoir Opinaca), diorite (Lac Ell), LCT pegmatite, and feldspar-phyric monzonite. The Cheechoo tonalite is an example of the variability of rock types that host traces of diopside, actinolite, and gold mineralization (Fig. 3g). Lithium-cesium-tantalum granitic pegmatite displays various textures and mineralogy, suggesting that important segregation processes occurred during the emplacement of the granitic melt and that these variations can probably be used as good indicators for distinguishing if the pegmatite is gold-bearing (Fig. 6d). Some of granitic pegmatite dykes show progressive evolution with paragneiss rocks and some appear more evolved (spodumene-bearing pegmatite), suggesting various sources (Cheechoo tonalite, migmatite). In addition, the feldspar-phyric monzonite (Fig. 3f) shows a spatial association with the North zone (Figs. 4c,f, 6).

The calcium-bearing metasomatism, present for more than 400 m around the ore zones, is sometimes fracture-controlled (Fig. 4a,e) and with evolving mineralogy, thickness of veins or replacement zones, style and sulphide content. The integration of such variations in the metasomatic footprint represents an exploration vector (Fig. 4), which, notwithstanding metamorphic grade, is comparable to many sediment-hosted gold deposits worldwide (Sillitoe and Bonham, 1990). Also, the deposit is located a few kilometres from a migmatitic domain where partial melting (Morfin et al., 2013) and exhumation processes (Vry et al., 2010) may have been involved in the production of metamorphic fluids.

CONCLUDING REMARKS

This study illustrates the complex tectonometamorphic framework affecting the Low Formation, the host of the bulk of the gold mineralization at the Roberto deposit, which includes a wide range of mineralization styles: i) stockwork of quartz, dravite veinlets with microcline, phlogopite, and sulphides; ii) replacement zones (microcline, phlogopite, dravite) with traces of pyrrhotite, arsenopyrite, and rare löllingite (Roberto zone); ii) quartz, diopside, schorl, arsenopyrite veins (East-Roberto zone); iv) atypical ore zones in quartz-feldspathic veinlets, high-grade quartz veins, high-grade paragneiss (North zone and Hanging-wall zone); and v) local gold-bearing LCT pegmatite. The underground mapping provides new insights to the geology of the first world-class gold deposit in the James Bay region:

- The strong metamorphic gradient documented in the northeastern part of the deposit extends at

depth, suggesting that metamorphic isograds have a moderate dip to the southwest and intersect the subvertical mineralized envelope at approximately 1 km depth.

- High-strain zones are associated with all the mineralization styles, including high-grade paragneiss at depth, suggesting that hydrothermal alteration assemblages could play a role in focussing strain increments.
- The diversity of mineralization styles is due to a combination of factors: i) the superposition of gold deposition events or remobilization; ii) structural events obliterating primary hydrothermal features, and iii) the higher metamorphic grade affecting multiple host rocks, leading to atypical hydrothermal assemblages in contrast to those of classical greenschist-facies Archean gold deposits (Goldfarb et al., 2005, Robert et al., 2005; Dubé and Gosselin, 2007).
- Magmatic activity is spatially associated with the contact between Opinaca and La Grande subprovinces.
- Gold mineralizing event(s) occurred between 2675 Ma (e.g. maximum age of Low Formation) and ca. 2600 Ma (e.g. preliminary age of a gold-bearing pegmatite), a time span during which the turbiditic sequence was deposited, deeply buried, and exhumed.

IMPLICATIONS FOR EXPLORATION

The contact between the Opinaca and the La Grande subprovinces is a first-order gold exploration metallotect in the James Bay region (Fig. 1; Ravenelle et al., 2010; this study). Typified by a high metamorphic gradient (Gauthier et al., 2007), it has probably focused hydrothermal circulation, which occurred between deposition of the Low Formation deposition at <2675 Ma (Ravenelle et al., 2010) and the crystalization of a gold-bearing pegmatite at 2600 Ma (this study). During this 75 Ma time span, the turbiditic rocks were deeply buried, strongly tilted, and metamorphosed to amphibolite grade leading to the generation of aqueous fluids (from metapelitic units, mainly with muscovite or biotite breakdown mainly in metapelitic units). The discovery of gold mineralization hosted by the Cheechoo tonalite (Figs. 1b, 3g) suggests a second distinct gold mineralizing event in close proximity to the Roberto deposit, as proposed by Ravenelle et al. (2010). In terms of host rocks, the occurrence of aluminosilicate-bearing greywacke (Figs. 2, 4a), local conglomerate, and north-trending bedding, combined with the evidence of calcium-bearing metasomatism (Fig. 4a) are important geological parameters for gold exploration. Coupled with the proximity of the contact between the two subprovinces, west- and north-trending high-strain zones and kilometre-scale polyphase folds (Figs. 2, 4a) are structural targets for gold in James Bay region (Ravenelle et al., 2010; Ravenelle, 2013; this study).

FUTURE WORK

A lithogeochemical program to define the hydrothermal footprint of the deposit is currently underway in collaboration with Goldcorp Inc.'s exploration team and MERN (Ministère de l'Énergie et des Ressources naturelles). In addition, LA-ICP-MS mineral mapping is underway on gold-bearing sulphide assemblages. Magmatism (feldspar porphyry dykes, monzonite, granitic dykes) is also being geochemically investigated for its possible (active or passive) role on the genesis of the deposit. U-Pb geochronology and geothermobarometry is also being completed to constrain the pressure-temperature-time path of the Low Formation and characterize the long-lived metamorphic event. Data from some gold exploration projects around the Éléonore mine (e.g. Cheechoo, Éléonore Sud, Vieux Camp) will be integrated into a geological model.

ACKNOWLEDGEMENTS

Goldcorp Inc., Éléonore mine is gratefully acknowledged for logistics during fieldwork and underground access (staff from Geology Exploration Department and Geology Mine department, especially François Pulinckx, Catherine Vellet and David Bélisle), scholarship funding, and scientific support for the geology and new data obtained through mine production activity. Eric Fournier (Exploration Geologist at Goldcorp Inc.) is particularly thanked for technical, logistical, and scientific support on ArcGIS software. We are grateful to Julie Doyon, Luc Théberge, Peter Lauder, and Martin Perron for many constructive and enthusiastic discussions related to this scientific research. Ressources Sirios is also thanked for constructive discussions and sharing their knowledge on the geology of the Cheechoo project. INRS ETE, GSC, FRQNT (Fonds de recherche du Québec – Natures et technologies) and NSERC (Natural Sciences and Engineering Research Council of Canada) are also thanked for a scholarship funding related to the BMP (Bourse en milieu pratique) Innovation funding. We are grateful to the reviewer, Sébastien Castonguay, for helpful comments that improved the clarity of the manuscript.

REFERENCES

Aucoin, M., Beaudoin, G., Creaser, R.A., and Archer, P., 2012. Metallogeny of the Marco zone, Corvet Est, disseminated gold deposit, James Bay, Quebec, Canada; Canadian Journal of Earth Sciences, v. 49, p. 1154–1176.

Bandyayera, D. and Fliszár, A., 2007. Géologie de la région de la baie Kasipaskatch (33C09) et du lac Janin (33C16); Ministère des Ressources naturelles et de la Faune du Québec, RP 2007-05, 15 p.

Bandyayera, D., Rhéaume, P., Maurice, C., Bédard, E, Morfin, S., and Sawyer, E.W., 2010. Synthèse géologique du Secteur du Réservoir Opinaca, Baie-James; Ministère des Ressources naturelles et de la Faune du Québec, RG 2010-02, 44 p.

Barnicoat, A.C., Fare, R.J., Groves, D.I., and McNaughton, N.J., 1991. Syn-metamorphic lode-gold deposits in high-grade Archean settings; Geology, v. 19, p. 921–924.

Beauchamp, A-M., Dubé, B., Malo, M., McNicoll, V.J., Archer, P., Lavoie, J., and Chartrand, F., 2015. Geology, mineralization and alteration of the turbidite-hosted Mustang Au showing, Lower Eastmain greenstone belt, Superior Province, Quebec, *In:* Targeted Geoscience Initiative 4: Contributions to the Understanding of Precambrian Lode Gold Deposits and Implications for Exploration, (ed.) B. Dubé and P. Mercier-Langevin; Geological Survey of Canada, Open File 7852, p. 227–243.

Bécu, V., Ravenelle, J-F., Malo, M., Dubé, B., Gauthier, M., and Simoneau, J., 2007. Résultats préliminaires de l'étude de la minéralisation Cu-Au-Ag de l'indice du Lac Ell et de ses implications sur la genèse du gisement d'or Roberto, propriété Éléonore, Baie James; Rapport d'étape DIVEX, SC21, 40 p. http://www.divex.ca/projets/sc21.php

Card, K.D. and Ciesielski, A., 1986. Subdivisions of the Superior Province of the Canadian Shield; Geoscience Canada, v. 13, p. 5–13.

Černý, P., 1991. Fertile granites of Precambrian rare-element pegmatite fields: is geochemistry controlled by tectonic setting or source lithologies?; Precambrian Research, v. 51, p. 429–468.

Černý, P. and Ercit, T.S., 2005. The classification of granitic pegmatites revisited; The Canadian Mineralogist, v. 43, p. 2005–2026.

David, J., 2005. Rapport d'analyses géochronologiques sur des diorites provenant du secteur de la rivière Eastmain – avril 2005; Rapport interne, Virginia Mines Inc., 9 p.

David, J., Davis, D.W., Bandyayera, D., Pilote, P., and Dion, C., 2009. Datations U-Pb effectuées dans les sous-provinces de l'Abitibi et de La Grande en 2006-2007; Ministère des Ressources naturelles et de la Faune du Québec, RP 2009-02, 17 p.

Dubé, B. and Gosselin, P., 2007. Greenstone-hosted quartz-carbonate vein deposits, *In:* Mineral Deposits of Canada: A Synthesis of Major Deposit Types, District Metallogeny, the Evolution of Geological Provinces, and Exploration Methods, (ed.) W.D. Goodfellow; Geological Association of Canada, Mineral Deposits Division, Special Publication, No. 5, p. 49–73.

Dubé, B., Balmer, W., Sanborn-Barrie, M., Skulski, T., and Parker, J., 2000. A preliminary report on amphibolite facies, disseminated replacement-style mineralization at the Madsen gold mine, Red Lake, Ontario; Geological Survey of Canada, Current Research 2000-C17, 12 p.

Dubé, B., Mercier-Langevin, P., Castonguay, S., McNicoll, V., Pehrsson, S.J., Bleeker, W., Schetselaar, E.M., and Jackson, S., 2011a. Targeted Geoscience Initiative 4. Lode gold deposits in ancient, deformed and metamorphosed terranes – footprints and exploration implications: a preliminary overview of themes, objectives and targeted areas, *In:* Summary of field work and other activities 2011; Ontario Geological Survey, Open File Report 6270, p. 38-1 to 38-10.

Dubé, B., Ravenelle, J.-F., McNicoll, V., Malo, M., Nadeau, L., Creaser, R.A., and Simoneau, J., 2011b. The world-class Roberto gold deposit, Éléonore property, James Bay area, Superior province, Quebec: Insights from geology and geochronology, *In:* Program with Abstracts; Geological Association of Canada-Mineralogical Association of Canada-Society of Economic Geologists-Society for Geology Applied to Mineral Deposits (GAC-MAC-SEG-SGA) joint meeting, Ottawa, May 25-27, 2011, v. 34, p. 55.

Fontaine, A., Dubé, B., Malo, M., McNicoll, V., and Brisson, T., 2014. Géologie et caractéristiques structurales du gisement aurifère Roberto, Propriété Éléonore, Province du Supérieur, Baie-James, Québec, Canada, *In:* Abstracts; Québec Mines 2014, Ministère de l'Énergie et des Ressources naturelles du Québec, Québec, 17-20 novembre, 2014, DV 2014-04, p. 135.

Franconi, A., 1978. La bande volcanosédimentaire de la rivière Eastmain Inférieure; Ministère des richesses naturelles du Québec, DPV-574, 184 p.

Gauthier, M., 2000. Styles et répartition des gîtes métallifères du territoire de la Baie-James (Québec); Chronique de la recherche minière, N 539, p. 17–61.

Gauthier, M., Trépanier, S., and Gardoll, S., 2007. Metamorphic gradient: A regional-scale area selection criterion for gold in the northeastern Superior province, eastern Canadian Shield; Society of Economic Geologists Newsletter, v. 69, p. 1, 10–15.

Goldcorp, 2014. Reserves & Resources; http://www.goldcorp.com/English/Investor-Resources/Reserves-and-Resources/default.aspx (February 9th, 2015).

Goldfarb, R.J., Baker, T., Dubé, B., Groves, D.I., Hart, C.J.R., Robert, F., and Gosselin, P., 2005. World distribution, productivity, character, and genesis of gold deposits in metamorphic terranes, *In:* 100th Anniversary Volume, (ed.) J.W. Hedenquist, J.F.H. Thompson, R.J. Goldfarb, and J.P. Richards; Society of Economic Geologists, p. 407–450.

Gosselin, P. and Dubé, B., 2005a. Gold deposits and gold districts of the world; Geological Survey of Canada, Open File 4893, 1 sheet.

Gosselin, P. and Dubé, B., 2005b. Gold deposits of the world: distribution, geological parameters and gold content: Geological Survey of Canada, Open File 4895, 214 p., 1 CD-ROM.

Goutier, J. and Dion, C., 2004. Géologie et minéralisation de la Sous-province de La Grande, Baie-James, Dans: Résumés des conférences et des photoprésentations; Québec Exploration 2004, Ministère des Ressources naturelles et de la Faune du Québec, Québec, 22-25 novembre, 2004, DV 2004-06, p. 21.

Goutier, J., Dion, C., Ouellet, M.C., Mercier-Langevin, P., and Davis, D.W., 2001. Gélogie de la Colline Masson, de la Passe Awapakamich, de la Baie Caribellet et de la Passe Pikwahipanan (SNRC 33F/09, 33F/15 et 33F/16); Ministère des Ressources naturelles du Québec, RG-2000-10, 67 p.

Groves, D.I., Goldfarb, R.J., Gebre-Mariam, M., Hagemann, S.G., and Robert, F., 1998. Orogenic gold deposits: A proposed classification in the context of their crustal distribution and relationship to other gold deposit types; Ore Geology Reviews, v. 13, p. 7–27.

Henry, D.J., Guidotti, C.V., and Thomson, J.A., 2005. The Ti-saturation surface low-to-medium pressure metapelitic biotites: Implications for geothermometry and Ti-substitution mechanisms; American Mineralogist, v. 90, p. 316–328.

Hodgson, C.J., 1993. Mesothermal lode-gold deposits, *In:* Mineral Deposit Modelling, (ed.) R.V. Kirkham, W.D. Sinclair., R.I. Thorpe, and J.M. Duke; Geological Association of Canada, Special Paper 40, p. 635–678.

Holdaway, M.J., 2000. Application of new experimental and garnet Margules data to the garnet-biotite geothermometer; American Mineralogist, v. 85, p. 881–892.

Kisters, A.F.M., Kolb, J., and Meyer, F.M., 1998. Gold mineralization in high-grade metamorphic shear zones of the Renco Mine, southern Zimbabwe; Economic Geology, v. 93, p. 587–601.

Mercier-Langevin, P., Daigneault, R., Goutier, J., Dion, C., and Archer, P., 2012. Geology of the Archean intrusion-hosted La-Grande-Sud Au-Cu prospect, La Grande subprovince, James Bay Region, Québec; Economic Geology, v. 107, p. 935–962.

Morfin, S., Bandyayera, D., and Sawyer, E.W., 2013. Large volumes of anatectic melt retaine in granulite facies migmatites: An injection complex in northern Quebec; Lithos, v. 168-169, p. 200–218.

McCuaig, T.C., Kerrich, R., Groves, D.I., and Archer, N., 1993. The nature and dimensions of regional and local gold-related hydrothermal alteration in tholeiitic metabasalts in Norseman goldfields: The missing link in a crustal continuum of gold deposits?; Mineralium Deposita, v. 28, p. 420–435.

Moukhsil, A., Legault, M., Boily, M., Doyon, J., Sawyer, E., and Davis, D.W., 2003. Synthèse géologique et métallogénique de la ceinture de roches vertes de la Moyenne et de la Basse-Eastmain (Baie-James); Ministère des Ressources naturelles, de la Faune et des Parcs du Québec, ET 2002-06, 55 pages, 1 plan.

Neumayr, P., Cabri, L.J., Groves, D.I. Mikucki, E.J., and Jackman, J.A., 1993. The mineralogical distribution of gold and relative timing of gold mineralization in two Archean settings of high metamorphic grade in Australia; The Canadian Mineralogist, v. 31, p. 711–725.

Percival, J.A., 2007. Geology and metallogeny of the Superior Province, Canada, *In:* Mineral Deposits of Canada: A Synthesis of Major Deposit Types, District Metallogeny, the Evolution of Geological Provinces, and Exploration Methods, (ed.) W.D. Goodfellow; Geological Association of Canada, Mineral Deposits Division, Special Publication, No. 5, p. 903–928.

Phillips, G.N. and Powell, R., 2009. Formation of gold deposits: Review and evaluation of the continuum model; Earth-Sciences Reviews, v. 94, p. 1–21.

Poulsen, K.H., Robert, F., and Dubé B., 2000. Geological classification of Canadian gold deposits; Geological Survey of Canada, Bulletin 540, 106 p.

Ramsay, J. and Huber, M., 1987. The techniques of modern structural geology: Folds and fractures; Academic Press, London, 391 p.

Ravenelle J.-F., 2013. Amphibolite Facies Gold Mineralization: An example from the Roberto deposit, Eleonore property, James Bay, Quebec; Ph.D. thesis, Institut national de la recherche scientifique, Centre Eau Terre Environnement, Québec, Quebec, 283 p.

Ravenelle, J.-F., Dubé, B., Malo, M., McNicoll, V., and Nadeau, L., 2009. Geology of the amphibolite-facies world-class Roberto gold deposit, Eleonore property, James Bay, Canada, *In:* Proceeding; Tenth Biennial SGA Meeting, Townsville, Australia, August 17-20, 2009, p. 59–61.

Ravenelle J.-F., Dubé B., Malo M, McNicoll V., Nadeau L., Simoneau J., 2010. Insights on the geology of the world-class Roberto gold deposit, Eléonore property, James Bay area, Québec; Geological Survey Canada, Current Research 2010-1, 26 p.

Robert F., Poulsen K.H., Cassidy K. F., Hodgson C.J., 2005. Gold metallogeny of the Superior and Yilgarn cratons, *In:* 100th Anniversary Volume, (ed.) J.W. Hedenquist, J.F.H. Thompson, R.J. Goldfarb, and J.P. Richards; Society of Economic Geologists, p. 1001–1033.

Ressources Sirios, 2014. Press release; http://sirios.com/fr/chee-choo, (December 8th, 2014).

Sillitoe R.H. and Bonham H.F., 1990. Sediment-hosted gold deposits: Distal products of magmatic-hydrothermal systems; Geology, v. 18, p. 157–161.

Stüwe, K., 1998. Tectonic constraints on the timing relationships of metamorphism, fluid production, and gold-bearing quartz vein emplacement; Ore Geology Reviews, v. 13, p. 219–228.

Thériault, R. and Beauséjour, S., 2012. Carte géologique du Québec – édition 2012; Ministère des Ressources naturelles du Québec, DV 2012-06, 8 p., 1 carte et données numériques.

Thompson, A.B. and Tracy, R.J., 1979. Model systems for anatexis of pelitic rocks. II. Facies series melting and reaction in the system $CaO\text{-}KAlO_2\text{-}NAlO_2\text{-}Al_2O_3\text{-}SiO_2\text{-}H_2O$; Contributions to Mineralogy and Petrology, v. 98, p. 257–276.

Thompson, P.H., 2003. Toward a new metamorphic framework for gold exploration in the Red Lake greenstone belt; Ontario Geological Survey, Open File Report 6122, 52 p.

Tomkins, A.G. and Mavrogenes, J.A., 2002. Mobilization of gold as a polymetallic melt during pelite anatexis at the Challenger deposit, South Australia: a metamorphosed Archean gold deposit; Economic Geology, v. 97, p. 1249–1271.

Tomkins, A.G., Pattison, D.R.M., and Zaleski, E., 2004. The Hemlo gold deposit, Ontario: an example of melting and mobilization of a precious metal-sulfosalt assemblage during amphibolite facies metamorphism and deformation; Economic Geology, v. 99, p. 1063–1084.

Tomkins, A.G., Frost, B.R., and Pattison, D.R.M., 2006. Arsenopyrite melting during metamorphism of sulfide ore deposits; The Canadian Mineralogist, v. 44, p. 1045–1062.

Vielzeuf, D. and Holloway J.R., 1988. Experimental determination of fluid-absent melting relations in the pelitic system: consequences for crustal differentiation; Contributions to Mineralogy and Petrology, v. 98, p. 257–276.

Vry J., Powell, R., Golden, K.M., and Petersen, K., 2010. The role of exhumation in metamorphic dehydration and fluid production; Nature Geoscience, v. 3, p. 31–35.